The AAPS Journal, Vol. 18, No. 3, May 2016 (© 2016)
DOI: 10.1208/s12248-016-9879-0

Research Article

The Population Pharmacokinetics of D-β-hydroxybutyrate Following Administration of (*R*)-3-Hydroxybutyl (*R*)-3-Hydroxybutyrate

Vittal Shivva,[1,4] Pete J. Cox,[2] Kieran Clarke,[2] Richard L. Veech,[3] Ian G. Tucker,[1] and Stephen B. Duffull[1]

Received 26 October 2015; accepted 21 January 2016; published online 18 February 2016

Abstract. The administration of ketones to induce a mild ketosis is of interest for the alleviation of symptoms associated with various neurological disorders. This study aimed to understand the pharmacokinetics (PK) of D-β-hydroxybutyrate (BHB) and quantify the sources of variability following a dose of (*R*)-3-hydroxybutyl (*R*)-3-hydroxybutyrate (ketone monoester). Healthy volunteers ($n = 37$) were given a single drink of the ketone monoester, following which, 833 blood BHB concentrations were measured. Two formulations and five dose levels of ketone monoester were used. A nonlinear mixed effect modelling approach was used to develop a population PK model. A one compartment disposition model with negative feedback effect on endogenous BHB production provided the best description of the data. Absorption was best described by two consecutive first-order inputs and elimination by dual processes involving first-order ($CL = 10.9$ L/h) and capacity limited elimination ($V_{max} = 4520$ mg/h). Covariates identified were formulation (on relative oral bioavailable fraction and absorption rate constant) and dose (on relative oral bioavailable fraction). Lean body weight (on first-order clearance) and sex (on apparent volume of distribution) were also significant covariates. The PK of BHB is complicated by complex absorption process, endogenous production and nonlinear elimination. Formulation and dose appear to strongly influence the kinetic profile following ketone monoester administration. Further work is needed to quantify mechanisms of absorption and elimination of ketones for therapeutic use in the form of ketone monoester.

KEY WORDS: D-β-hydroxybutyrate; exogenous ketosis; ketone monoester; pharmacokinetics; population models.

INTRODUCTION

There is increasing evidence of the therapeutic benefits of artificially induced mild ketosis in various disorders (1). Ketones are the endogenous products of fat metabolism and constitute D-β-hydroxybutyrate (BHB), acetoacetate (AcAc) and acetone. Ketones are produced in the liver as an evolutionary response to starvation and constitute a vital energy source when dietary glucose is unavailable. Amongst the ketones, BHB and AcAc are used as a source of energy by the heart, brain and skeletal muscle (2,3). In healthy individuals, blood concentrations of total ketones are generally less than 0.5 mmol/L (equivalent to 52.05 mg/L of BHB), whereas after prolonged fasting (e.g. for a week) blood ketone concentrations can be 5–7 mmol/L (equivalent to 520.5–728.7 mg/L of BHB) called starvation ketosis (4). Blood ketone concentrations in diabetic patients with ketoacidosis may exceed 25 mmol/L (5,6).

Induction of physiological ketosis, e.g. by administration of ketones, to yield blood concentrations of ketones equivalent to those in starvation ketosis, has been purported to have therapeutic benefit in a number of clinical conditions, such as epilepsy (7), neurodegenerative disorders (such as Alzheimer's (8) and Parkinson's diseases (9)). Investigations using preclinical animal models support potential of ketones in improving conditions of insulin resistance in the brain, a commonly associated factor with Alzheimer's disease (9,10). Induction of acute mild ketosis has been proposed for improving physical performance and cognitive function (11). Induction of mild ketosis can be achieved either by prolonged fasting or by consumption of a diet high in fat and low in carbohydrate. Diets may also elevate plasma concentrations of triglycerides and cholesterol, which carries a risk of complications, such as vascular disorders and diabetes (12). A novel means of inducing ketosis is by administration of the ketone monoester ((*R*)-3-hydroxybutyl (*R*)-3-hydroxybutyrate), which is broken down by esterases to form BHB *in vivo* (13). The ketone monoester is expected to undergo complete enzymatic hydrolysis following oral intake to release BHB and butane-1,3-diol. The carboxylesterases involved are

Electronic supplementary material The online version of this article (doi:10.1208/s12248-016-9879-0) contains supplementary material, which is available to authorized users.

[1] School of Pharmacy, University of Otago, P.O. Box 56, Dunedin, 9054, New Zealand.
[2] Department of Physiology, Anatomy and Genetics, University of Oxford, Oxford, UK.
[3] Laboratory of Metabolic Control, NIAAA/NIH, Rockville, Maryland, USA.
[4] To whom correspondence should be addressed. (e-mail: vittal.shivva@otago.ac.nz;)

expressed throughout the gastrointestinal tract, liver and blood. R-1,3-butanediol is further metabolised in the liver and blood to produce BHB (14,15). BHB in the liver is metabolised to AcAc and acetone (16). BHB and AcAc in blood circulation are taken up by extra hepatic tissues and are used as energy source (17).

Several reports are available in the literature that describe the kinetics of ketones in humans following intravenous infusion (18–21). Most of these studies used tracer techniques involving infusion of small amounts of labelled BHB and AcAc, which do not alter normal physiological ketone concentrations. Recently, a preliminary study in healthy adults established the pharmacokinetics (PK), safety and tolerability following single and multiple drinks of the ketone monoester that produced ketone concentrations equivalent to starvation ketosis (13). In this study, ketones were administered in the form of the ketone monoester in a meal replacement drink in healthy adult volunteers. This study consisted of a single drink (140, 357 and 714 mg/kg of the ketone monoester) and a repeat drink administration (140, 357 and 714 mg/kg of the ketone monoester three times a day for 5 days) with the ketone monoester. This study reported plasma concentrations of BHB and AcAc. PK evaluation in this study was performed using the single dose administration data. Area under the plasma concentration-time curve (AUC_{inf}) for BHB were 1.09, 4 and 13 mM.h (113.5, 416.4 and 1353 mg.h/L) for 140, 357 and 714 mg/kg drink groups, respectively. The authors found the increase in AUC and C_{max} was more than dose proportional suggesting nonlinearity in the PK. Time for C_{max} (T_{max}) was in the range of 1.5 to 2.5 h, with increased T_{max} noted for high dose group. Clearance (CL/F) was ranged from 4179 to 11946 mg/mM.h (40.14 to 114.7 L/h), and the smaller dose had higher (~ 3 times) clearance. Due to limitations associated with the non-compartmental approach, a detailed understanding of the PK of ketones was not possible in this study.

The ratio of BHB and AcAc in blood during normal physiological ketone conditions is approximately unity (BHB:AcAc = 1:1). This ratio may rise up to 4 to 6 during excess blood ketone concentrations (such as under conditions of starvation ketosis), by means of a physiological compensatory mechanism to prevent metabolic acidosis (22). Thus, ketotic conditions (such as starvation ketosis) are associated with excessively high blood concentrations of BHB compared to AcAc and it is of great interest to explore and understand the PK of BHB, under such conditions. The present study aimed to describe and quantify the pharmacokinetics of BHB from orally administered ketone monoester and to identify and quantify sources of variability. The study objectives were (1) to develop a population PK model, (2) to describe absorption and elimination processes and to identify covariates that account for PK variability and (3) to provide a basis for the design of future studies on the catabolic disposition of the ketone monoester.

METHODS

The study was conducted at the University of Oxford, UK, as a part of ongoing investigations into the ketone monoester. It was approved by the Oxfordshire Research Ethics Committee and conducted in accordance with the guidelines of the Declaration of Helsinki. All participating subjects gave written informed consent.

Study Population

Healthy human volunteers ($n = 37$; 22 males and 15 females) consumed a single drink of the ketone monoester (see Supplemental materials and methods online). Two drink formulations were studied. Formulation 1 was a citrus-flavoured sports drink that was prepared in four dose levels of ketone monoester (192, 291, 395 and 573 mg/kg). Formulation 2 was a chocolate milkshake meal replacement preparation and consisted of one 500 mg/kg group (see Supplemental materials and methods online for calorific composition of formulations). All subjects received a single drink of the ketone monoester following an overnight fast, and blood samples were collected for analysis of BHB concentration. Dosing details and demographic details of the subjects are presented in Table I. Covariates for assessing variability in PK were formulation, dose, age, sex, weight (WT), lean body weight (LBW) and height. In this study, LBW was calculated according to the method of Janmahasatian *et al.* (23).

Samples and Assays

A rich sampling design was used in all dose groups. Capillary blood samples were collected before and every 15 min after the drink until the blood concentrations had returned to pre-drink concentrations of BHB (i.e. 0.1 to 0.2 mmol/L (10.41 to 20.82 mg/L)). For the 291, 395 (Formulation 1) and 500 mg/kg (Formulation 2) groups, the blood sampling schedule was before and at 0.25, 0.5, 0.75, 1, 1.25, 1.5, 1.75, 2, 2.25, 2.5, 2.75, 3, 3.25, 3.5, 3.75, 4, 4.25, 4.5, 4.75 and 5 h after the drink. Additional samples were collected in the 573 mg/kg group (Formulation 1) at 5.25, 5.5, 5.75, 6, 6.25, 6.5, 6.75 and 7 h post-drink. For the 192 mg/kg group (Formulation 1), the blood sampling schedule was before and after the drink at 0.08, 0.17, 0.25, 0.33, 0.42, 0.5, 0.75, 1, 1.25, 1.5, 1.75, 2, 2.25, 2.5, 2.75 and 3 h. Samples were collected from arterialised capillary droplet, either from a finger or earlobe, and analysed for BHB using FreeStyle Optium β ketone test strips (Abbott Diabetes Care, UK) (24). PK observations in this study were limited to BHB, and other analytes such as AcAc, acetone and precursors of ketones were not investigated. The lower limit of quantification (LLOQ) for BHB in this assay was 10.41 mg/L (0.1 mmol/L, conversion factor 104.1). The assay is highly selective for oxidation of BHB and has previously been validated. The specificity, selectivity, accuracy and precision of this analytical method have been reported (25,26). Accuracy of the assay was ranged from 91.4 to 107%, and precision (% CV) was ranged from 3.2 to 10.5%.

Population PK Modelling

The first-order conditional estimation with interaction method in NONMEM® version 7.2 was used to model the data (27). Additive, exponential and combined (additive + exponential) error models were explored to describe the residual unexplained variability as shown in Eq. 1:

$$y_{ij} = g(D_i, t_{ij}, \boldsymbol{\theta_i}) exp(\varepsilon_{1,ij}) + \varepsilon_{2,ij} \quad (1)$$

Table I. Formulation, Dosing and Demographic Data of the Subjects

Study Population	Formulation	Dose[a] (mg/kg)	Male/female[b]	Age[b, c] (years)	Height[b, c] (cm)	Weight[b, c] (kg)	Fat mass[b, c] (%)
37	Citrus-flavoured sports water preparation (Formulation 1)	573 (9)	5/4	27	181	71	19
(Healthy volunteers)			22/15	27	180	73	16
				(19—35)	(176—188)	(60—86)	(5.5—25)
				(19—36)	(173—189)	(52—96)	(5.5—27)
		395 (8)	3/5	25	178	68	17
				(21—35)	(173—189)	(52—87)	(8.6—27)
		291 (6)	3/3	34	179	74	11
				(20—36)	(176—186)	(55—96)	(5.5—23)
		192 (4)	3/1	31	180	85	15
				(20—33)	(177—189)	(65—87)	(14—17)
	Chocolate milkshake meal replacement preparation (Formulation 2)	500 (10)	8/2	24	181	75	15
				(21—32)	(174—189)	(61—84)	(6.5—22)

[a] Dose corresponds to ketone monoester, and the value in parentheses indicates the number of subjects
[b] Data stratified across dose/formulation and overall spread in the population, as shown in the table
[c] Data presented as median with the range in parenthesis

where y_{ij} represents the observed j^{th} concentration in the i^{th} individual, g is the functional form of the structural model that predicts the data, D_i is the dose administered to the i^{th} individual, t_{ij} represents the j^{th} time point in the i^{th} individual, $\boldsymbol{\theta_i}$ is the vector of parameter values for the i^{th} individual, $\varepsilon_{1,ij}$ represents the exponential random error and $\varepsilon_{2,ij}$ represents the additive random error. The additive and exponential errors were assumed to be identically, independently multivariate, normally distributed with mean of zero and a diagonal variance-covariance matrix ($\boldsymbol{\Sigma}$).

Heterogeneity or between-subject variance in parameter estimates was assumed to be distributed log normally and was modelled as shown in Eq. 2:

$$\theta_{ip} = \beta_p.exp\left(\eta_{ip}\right) \tag{2}$$

θ_{ip} represents the p^{th} parameter value in i^{th} individual, β_p is the population value for the p^{th} parameter, η_{ip} is the random effect for p^{th} parameter in the i^{th} individual. Random effects across the individuals in the population were assumed to be identically, independently multivariate normally distributed with means of zero and variance-covariance matrix ($\boldsymbol{\Omega}$).

Model Development

One, two and three compartment models with extravascular administration were assessed. All models were parameterised in terms of clearances (CL) and volumes of distribution (V). Zero-order, first-order absorption and multiple absorption sites models with and without lag time were explored for the absorption process. To account for data below limit of quantitation (BLQ), the M6 method (see Stuart Beal's methods to fit models to BLQ data) (28) was considered. Of note, the M3 method was tried initially but proved to be unstable (i.e. the model would reach a different objective function value following small perturbations in the initial parameter values). Finally, first-order and capacity limited (Michaelis-Menten kinetics) elimination processes were explored to describe the elimination of BHB. Basal concentrations were modelled to account for endogenous BHB. See B1 method proposed by Dansirikul *et al.* for estimation of baseline response (29). Turnover models were investigated to assess the effect of feedback inhibition on production of endogenous BHB.

Covariate Analysis

Assessment of covariates in this study was based on a predefined hierarchy. Covariates for assessment were chosen based on biological plausibility. Due to (statistical) nonlinearities inherent in PK models, the order of addition of covariates can affect their apparent statistical significance; hence, the order that they were considered is of importance. The predefined hierarchy based on our *a priori* belief about their likely contribution to the model was:

1. Formulation (on relative oral bioavailable fraction (F), first-order absorption rate constant (k_a) and lag time for oral absorption ($ALAG$))

2. Dose (on F and fraction absorbed from slow input site (f_{slowsite}))
3. Important phenotypic covariates such as WT, LBW (on CL, maximum rate of elimination by capacity limited pathway ($V_{\max}$) and V)
4. Other plausible phenotypic covariates such as age and sex (on CL, $V_{\max}$ and V)

Movement between the levels in the hierarchies for covariates was not allowed meaning a covariate considered at a specific level was not reconsidered whilst testing other covariates at lower levels. Within a hierarchy, standard forward selection and backward elimination were considered when there was more than one covariate (see Kumar *et al*. for similar method used in selection of covariates for Venlafaxine in overdose) (30).

Continuous covariates were assessed using nested covariate models. All continuous covariates such as dose, LBW and WT were centred either on their mean value (e.g. for Dose) or on a nominal value (e.g. 70 kg for WT) in the study as shown in Eq. 3 (for WT):

$$\theta_{ip} = \beta_p \cdot \left(\frac{WT}{70}\right)^{\beta_{cov}} \cdot exp\left(\eta_{ip}\right) \quad (3)$$

where β_p is the population value for the p^{th} parameter and β_{cov} represents the estimated exponent of covariate. Continuous covariates were assessed by linear and power relationships. Selection of the covariate was based on predefined criteria discussed below.

Model Selection and Evaluation

The following criteria were used in selecting models:

i. Stability of the model (i.e. the model would reach the same objective function value following small perturbations in the initial parameter values).
ii. Significant decrease in the objective function value (OBJV) i.e. 3.84 units (critical value from the chi-squared distribution with $p \leq 0.05$) for an additional parameter for nested models based on the likelihood ratio test (LRT).
iii. Parameter estimates are biologically plausible (e.g. $CL > 0$ L/h).
iv. A decrease in the residual unexplained variability.
v. A decrease in the between-subject variance of a parameter after addition of a covariate.

Amongst the above criteria, the first three were required and the last two were considered desirable. Finally, models were evaluated using a visual predictive check (VPC) (31). To construct a VPC, 1000 datasets were simulated using the model under evaluation and 10th (lower), 50th (median) and 90th (higher) percentiles of model predictions were plotted with the same percentiles of the original data. The percentiles of the model predictions also include the 95% confidence intervals around the model-predicted percentiles. For creating prediction-corrected VPCs, median predictions in each bin were used to normalise the observed and simulated concentrations in that bin (32). All VPCs were created in R (ver 3.0.2; The R project for Statistical Computing, Vienna, Austria).

RESULTS

Model Development

A one compartment disposition model was shown to describe the data well and was preferred over the other compartmental models that were considered. Residual variability was best described by a combined error model. Endogenous basal concentrations were modelled as approximately 68% of the total pre-drink samples were either equal to or greater than LLOQ of the assay for BHB. Estimation of the steady state basal value (BSL) in the model significantly decreased the OBJV (25 units, $p \leq 0.05$). BLQ data (blood concentrations less than 10.41 mg/L (0.1 mmol/L)) were modelled by the M6 method, where the first missing concentration was replaced by half of BLQ (5.21 mg/L (0.05 mmol/L)), and the remaining missing data omitted from the dataset. Exploration of the diagnostic plots (see Supplemental Fig. S1 online) revealed that formulation and dose greatly influenced the exposure and both were found to be statistically significant when included in the model prior to finalisation of the structural model (see covariate analysis below). Hence, a base model (structural model without any covariates) does not exist in this study. To study the influence on absorption, dose was included as covariate on the extent of absorption (on the relative oral bioavailable fraction 'F') and the rate of absorption via a dose-dependent fraction being absorbed from second/slow input site ($f_{\text{slow site}}$).

Elimination of BHB was found to be nonlinear as shown by an apparent convexity in the terminal phase in the log concentration-time plots (see Supplemental Fig. S2 online), and inclusion of this process as a Michaelis-Menten equation in the model resulted in a significant drop in the OBJV (589 units, $p \leq 0.05$). Finally, dual elimination processes (first-order and Michaelis-Menten) provided the best fit to the data (a further drop in OBJV by 63 units, $p \leq 0.05$). A negative feedback process on endogenous ketogenesis was considered as a turnover model and was expressed in the ordinary differential equations (Eq. 4) shown later.

Diagnostic plots revealed that greater than 50% of the individuals showed multiple peaks in the profiles (see Supplemental Fig. S3 online). Subjects from higher dose groups showed flattening of the concentration-time profiles at around the time of maximum concentration (see Supplemental Fig. S2 and S3 online). In order to explore the influence of possible absorption profiles in the model, deterministic simulations were performed (see Supplemental Fig. S4 online) in MATLAB® (ver R2012a; The MathWorks Inc., MA, US). These simulated profiles were compared with the empirical data. Dual first-order input (fast and slow absorption sites) with linear dose effect on f_{slowsite} showed similar trends to the observations in the empirical data. Inclusion of this absorption process significantly improved the model fit (drop in OBJV by 58 units, $p \leq 0.05$), which was superior to parallel and sequential mixed order absorption models. Inclusion of lag time on input from slow absorption site further improved the model fit (drop in OBJV by 8 units, $p \leq 0.05$). The final model is shown as a schematic in Fig. 1.

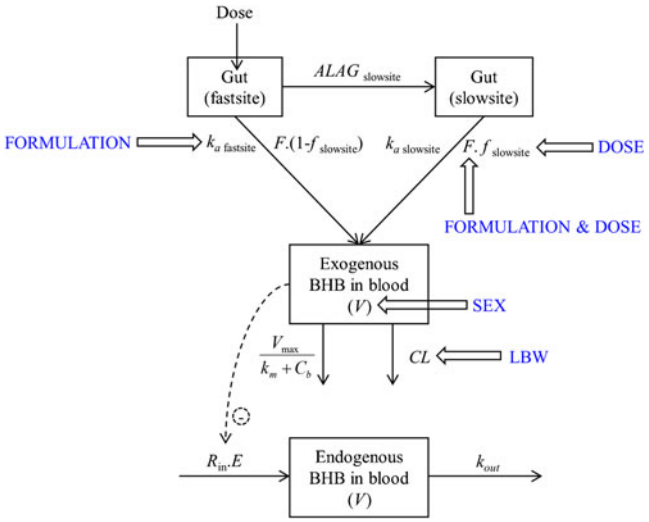

Fig. 1. Structure of the final population PK model. $k_{a\ \text{fastsite}}$ is absorption rate constant from fast input site and $k_{a\ \text{slowsite}}$ is absorption rate constant from slow input site. F is the oral relative bioavailable fraction for BHB following ketone monoester ingestion, f_{slowsite} is fraction absorbed from slow input site, $ALAG_{\text{slowsite}}$ is lag time for absorption from slow input site, R_{in} is rate of endogenous production, E is negative feedback effect of circulating BHB concentration on endogenous production, V is apparent volume of distribution, CL is first-order clearance, $V_{\max}$ is the maximum rate by capacity limited elimination, k_{m} is Michaelis-Menten constant and C_{b} is concentration of BHB in blood. Formulation, dose, sex and LBW are the covariates on fixed effects parameters as shown in the figure

Covariate Analysis

Formulation on F (drop in OBJV by 19 units, $p \le 0.05$) and dose on F and f_{slowsite} (drop in OBJV by 61 units, $p \le 0.05$) were included as covariates prior to the finalisation of the structural model. Formulation was also found to have a significant influence on the first-order absorption rate constant from the fast input site ($k_{a\ \text{fastsite}}$), but not on the absorption rate constant from the slow input site ($k_{a\ \text{slowsite}}$) or the lag time for absorption from slow input site ($ALAG_{\text{slowsite}}$). The effect of LBW on CL was modelled by a power function, and adding this covariate resulted in a 61% drop in the between subject variance of CL (drop in OBJV by 14 units $p \le 0.05$). The estimated exponent for LBW on CL of 2.09 was significantly different from the commonly accepted value of the allometric exponent (0.75). Neither WT nor LBW was found to have significant influence on $V_{\max}$ or V. Sex was found to be an influential covariate on V (21% drop in the between subject variance and a 5-unit drop in OBJV ($p \le 0.05$), and females had a lower volume of distribution (0.77 fractions of the volume of distribution in males).

Final Population PK Model

The final population PK model was a one-compartment disposition model with two first-order inputs and dual elimination processes involving first-order and Michaelis-Menten elimination with negative feedback effect on endogenous production of BHB. Ordinary differential equations (ODEs) for the final population PK model were as shown in Eq. 4:

$$\begin{aligned}
&\frac{dA_1}{dt} = -k_{a\ fastsite}\cdot F\cdot A_1 && ;A_{1(0)} = (1-f_{slowsite})\cdot Dose\\
&\frac{dA_2}{dt} = ALAG_{slowsite} - k_{a\ slowsite}\cdot F\cdot A_2 && ;A_{2(0)} = f_{slowsite}\cdot Dose\\
&\frac{dA_3}{dt} = k_{a\ fastsite}\cdot F\cdot A_1 + k_{a\ slowsite}\cdot F\cdot A_2 \\
&\qquad -CL\cdot C_3 - \frac{V_{max}}{k_m + C_3}\cdot C_3 && ;A_{3(0)} = 0;\ C_3 = \frac{A_3}{V}\\
&\frac{dA_4}{dt} = R_{in}\cdot\left(\frac{1}{1+e^{(-(INT+SLP\cdot C_3))}}\right) - k_{out}\cdot A_4 && ;A_{4(0)} = BSL\cdot V\\
&\text{here } R_{in} = BSL\cdot CL,\ \ k_{out} = \frac{CL}{V},\quad C_4 = \frac{A_4}{V}
\end{aligned} \tag{4}$$

where, A_1 and A_2 correspond to amounts in fast and slow input sites, respectively, A_3 corresponds to the amount in the measured compartment (blood) from exogenous administration, A_4 corresponds to the amount of BHB in blood related to endogenous ketone production. Note that the ester is converted rapidly to BHB via enzymatic reactions in the gut and the systemic circulation. The blood BHB concentration is sum of exogenous (C_3) and endogenous (C_4) BHB concentrations, R_{in} is the rate of production (in mg/h) of endogenous BHB, INT is the intercept and SLP is the slope of the linear prediction in the function that shows negative feedback effect on endogenous production (drop in OBJV by 30 units, $p \le 0.05$). A negative feedback, $E_{\max}$ model was also tested; however, an expit was used for this process based on statistical criterion (smaller OBJV). The final population PK model with covariates is shown in Fig. 1. Although, biologically, the total drug ($C_{\text{total}} = C_3 + C_4$) is the driving force for feedback inhibition, a simplifying initial steady-state assumption was made in modelling the data that the steady state-production rate and elimination rate (product of the elimination rate constant and the amount of BHB in endogenous compartment (A_4)) were equal. When we make this assumption, the initial condition for feedback/endogenous compartment in the absence of exogenously administered ketone simplifies to the ratio of R_{in} and k_{out}. Therefore, the ODE for the endogenous compartment then simplifies to (under no feedback effect) as shown in Eq. 5:

$$\frac{dA_4}{dt} = R_{in} - k_{out}\cdot A_4 \qquad A_{4(0)} = \frac{R_{in}}{k_{out}} \tag{5}$$

Model estimated population parameters from the final PK model are presented in Table II. The relative standard error (% RSE) for all fixed effect parameters other than slope and intercept of the linear function in the negative feedback model and coefficient of dose on F were ≤ 50%. The CV% for all random effects parameters, except the random effects on BSL, was less than 50%.

Table II. Covariate Models and Parameter Estimates from the Final Population PK Model

Covariate models	
$f_{slowsite} = \beta_{f\ slowsite} \cdot \left(\frac{DOSE}{31184}\right)$	
$f_{slowsite}$ was constrained between 0, 1 using: $f_{slowsite} = \frac{1}{1+e^{-(f_{slowsite})}}$	
$F = \beta_{F\_formulation} + \beta_{coefficient\_DOSE\_F} \cdot \left(\frac{DOSE}{31184}\right)$	
F was constrained between 0, 1 using: $F = \frac{1}{1+e^{-(F)}}$	
$CL = \beta_{CL} \cdot \left(\frac{LBW}{70}\right)^{\beta_{coefficient\_LBW\_CL}}$	
$V = \beta_V \cdot \beta_{coefficient\_SEX\_V}$	
Parameter	Population estimate (% RSE)[a]
Structural parameters	
β_{CL} (L/h)	10.9 (18.7)
V_{max} (mg/h)	4520 (20.3)
k_m (mg/L)	52.7 (41.2)
β_V (L)	12.5 (16.7)
k_a fastsite_formulation 1[b] (h^{-1})	3.28 (13.1)
k_a fastsite_formulation 2[c] (h^{-1})	2.36 (16.5)
k_a slowsite (h^{-1})	0.54 (18.6)
$ALAG$ slowsite (h)	0.62 (3.80)
BSL (mg/L)	7.23 (14.9)
SLP	−0.051 (345)
INT	−15.5 (483)
Covariate effects	
$\beta_{f\ slowsite}$	0.36 (50.8)
$\beta_{F\_formulation}$	(formulation 1[b], fixed) 1 (formulation 2[c]) 0.37 (52.0)
$\beta_{coefficient\_DOSE\_F}$	−0.18 (144)
$\beta_{coefficient\_LBW\_CL}$	2.09 (43.8)
$\beta_{coefficient\_SEX\_V}$	(males, fixed) 1 (females) 0.77 (11.6)
Between subject variance (BSV) as % CV[d]	
BSV_{CL}	33.5 (45.4)
BSV_{Vmax}	19.7 (41.5)
BSV_{km}	54.3 (40.0)
BSV_V	30.7 (30.5)
BSV_{BSL}	52.8 (57.7)
Residual variability	
σ_{prop} (CV %)	16.2 (10.8)
σ_{add} (mg/L)	3.63 (33.9)

β population parameter estimate, CL first-order clearance, V_{max} maximum rate by capacity limited elimination, k_m Michaelis-Menten constant, V apparent volume of distribution, k_a absorption rate constant, $ALAG$ lag time for absorption, BSL basal concentration, SLP slope of linear prediction in expit, INT intercept of linear prediction in expit, f slowsite, fraction absorbed from slow input site (fraction absorbed from the fast site is 1—f slowsite), F oral relative bioavailable fraction, σ_{prop} standard deviation of the proportional error, σ_{add} standard deviation of the additive error

[a] Relative standard error (% RSE) = (standard error/mean value) × 100

[b] Citrus-flavoured sports water preparation

[c] Chocolate milkshake meal replacement preparation

[d] Coefficient of variation (% CV) = (variance)$^{0.5}$ × 100

The goodness-of-fit plots for the final population PK model are presented in Fig. 2. The plots indicate that the model described the data well. Good agreement was seen between observed *versus* population-predicted concentrations and observed *versus* individual-predicted concentrations, indicating a good fit with the data clustered around the line of identity. No systematic trends suggesting model misspecification were observed in residual plots and ε-shrinkage (33) was less than 10%.

Figure 3 presents the prediction-corrected VPC for the final model based on 10th, 50th and 90th percentiles of the observed and predicted concentrations of BHB. The lower and median percentiles of the model prediction showed good agreement with the observed data. The model prediction was slightly higher at the upper percentile compared to the observed data, although the 95% confidence interval around this prediction interval includes the observed percentile. Overall, VPCs show that the final population PK model was able to represent the data well.

VPCs across the dose levels tested in the study are presented in Fig. 4. Good agreement of the model prediction was observed with the data across the lower-dose groups (Fig. 4a to 4c) except the median prediction for the 291 mg/kg dose group (Fig. 4b). In the case of higher-dose groups, model prediction showed good agreement with the data at lower and median percentiles. Though there was slight over prediction at upper percentiles in higher-dose groups, the model was able to capture the trend of double peaks (Fig. 4d and 4e).

DISCUSSION

In this study, we have developed a population PK model that describes the disposition of D-β-hydroxybutyrate following a single drink of (*R*)-3-hydroxybutyl (*R*)-3-hydroxybutyrate. The PK of BHB appears to be complicated as a result of complex absorption processes involving multiple absorption sites, nonlinear and linear elimination and feedback mechanisms affecting endogenous production.

Literature evidence related to the metabolism of the ketone monoester after oral ingestion and information on endogenous ketogenesis were collated and presented as a schematic in Fig. 5. The ketone monoester is known to undergo enzymatic hydrolysis by carboxylesterases expressed throughout the gut wall, liver, blood and other tissues (14). One of the resulting products of ester breakdown, butane-1,3-diol, then undergoes sequential stepwise oxidation by alcohol dehydrogenase and aldehyde dehydrogenase in the liver to produce BHB (34). Conversion of BHB to other ketones in the liver and further utilisation in the extra hepatic tissues is similar to the endogenous pathway of ketogenesis (16) and ketolysis (17). Circulating ketones are usually taken up either by extra hepatic tissues to be utilised as an energy source or excreted unchanged by the kidneys or as acetone in the lungs. This schematic represents the likely complexity associated with the PK of BHB. Although the mechanism of ketone monoester breaks down *in vivo* is understood, it was not possible in this study to develop a more mechanistic population model due to lack of data of other ketone forms.

Multiple peaks in the profiles of some subjects (see Supplemental Fig. S3 online) and an apparent flattening of the concentration-time profiles in higher-dose groups (see Supplemental Fig. S2 online) suggest the presence of a multiple spacial and/or temporal aspects to absorption. The shape of the concentration-time profiles of BHB was comparable to γ-hydroxybutyate, a substrate of monocarboxylate

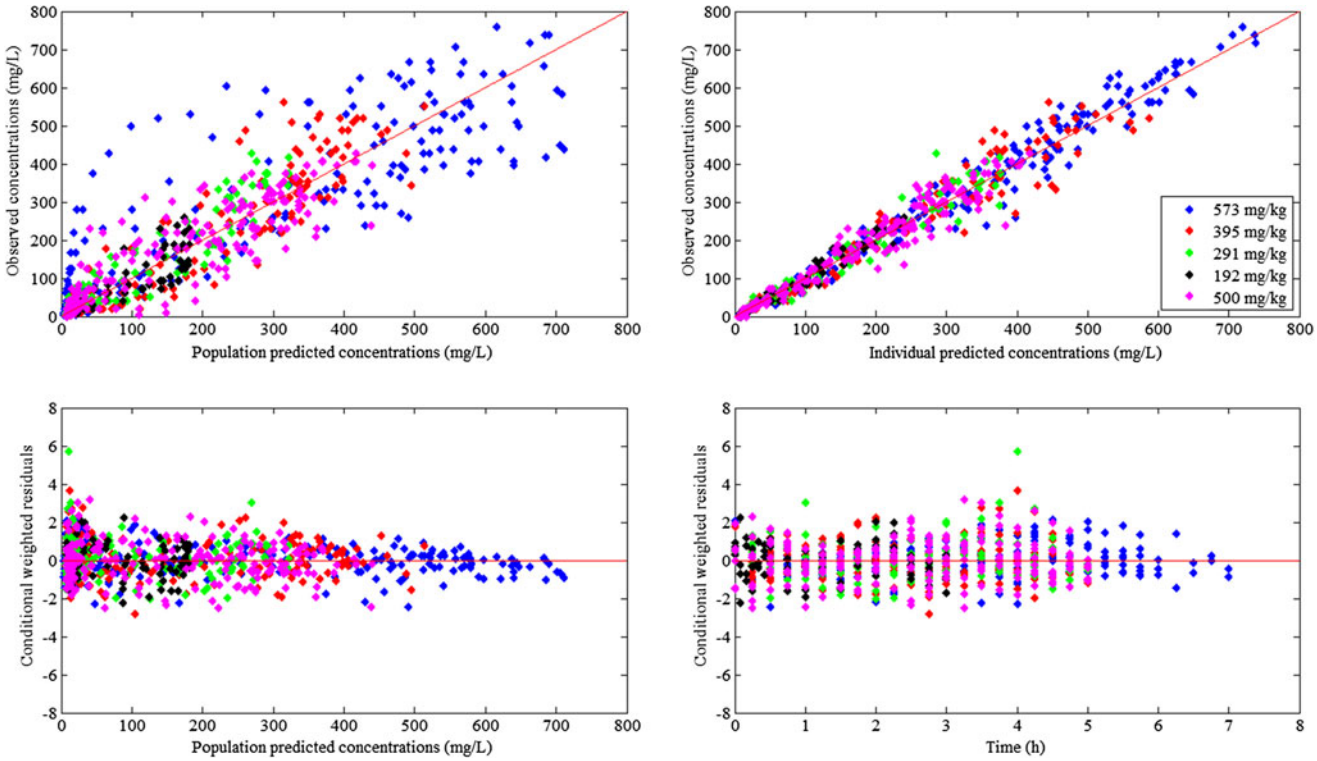

Fig. 2. Goodness-of-fit plots showing the observed *versus* population-predicted (*top left*) and individual-predicted concentrations (*top right*), conditionally weighted residuals *versus* population predicted (*bottom left*) and time (*bottom right*) from the final population PK model

transport (MCT) proteins (35). Possible mechanisms could include multiple absorption sites, the formation of temporary poorly soluble complexes, or enterohepatic circulation (although, given the low molecular weight of BHB (104.1 Da), this mechanism may be unlikely). The data in this study were unable to delineate potential mechanisms. A major portion of the administered monoester is expected to be absorbed as BHB by an active process involving MCTs, which are expressed throughout the gut wall (36). Expression of these transport proteins (MCT1 on the apical side, MCT4 and MCT5 on the basolateral side) has been shown to vary, potentially increasing, along the length of the colon (37). Substrate affinity and capacity of these transporters vary widely, and it is expected that saturation of these transporters at different sites will occur at different times, depending on pH and concentration of BHB at specific site (38,39). Variability in expression of transport proteins across the length of the gut supports the dual input sites for BHB in this model. Further studies are required to understand the absorption mechanisms of BHB.

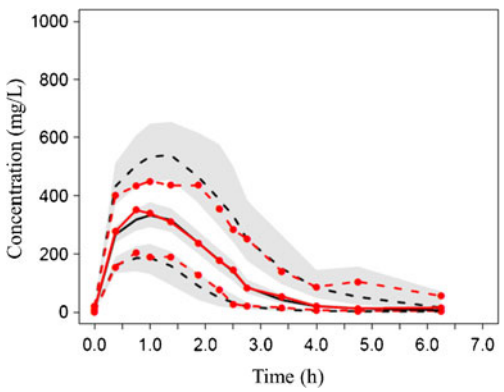

Fig. 3. Prediction-corrected VPC for the final population PK model showing 10th, 50th and 90th percentiles of the observed and model predicted data. *Dashed dotted lines* and *solid dotted line* represent percentiles of the observed data (*red lines*). *Dashed lines* and *solid line* represent median of percentiles of model predictions (*black lines*), and *shaded grey area* represent 95% confidence interval around each percentile from the model predictions

Elimination of BHB appears to be complicated, and modelling the processes suggested quantitatively that at least two dominant mechanisms (first-order and capacity limited elimination) contribute to its overall metabolism and excretion. Literature reported processes for elimination of ketones include (1) irreversible conversion of AcAc to acetone (via decarboxylation) in the blood and the liver, to be excreted from the lungs, (2) renal elimination of unchanged BHB and AcAc, which escape tubular reabsorption in the kidneys (18) and (3) uptake and consumption to produce energy (ATP) via the citric acid cycle in peripheral tissues such as the brain, skeletal muscle and heart (40). These known mechanisms of consumption and elimination support the quantitatively different mechanisms of elimination that were observed for BHB here. Under normal conditions, when the concentrations of circulating blood ketones are low (< 0.5 mmol/L (< 52.05 mg/L)), it is expected that elimination would follow a first-order process (concentrations being less than the empirical k_m of 52.7 mg/L, found in this study), whereas under

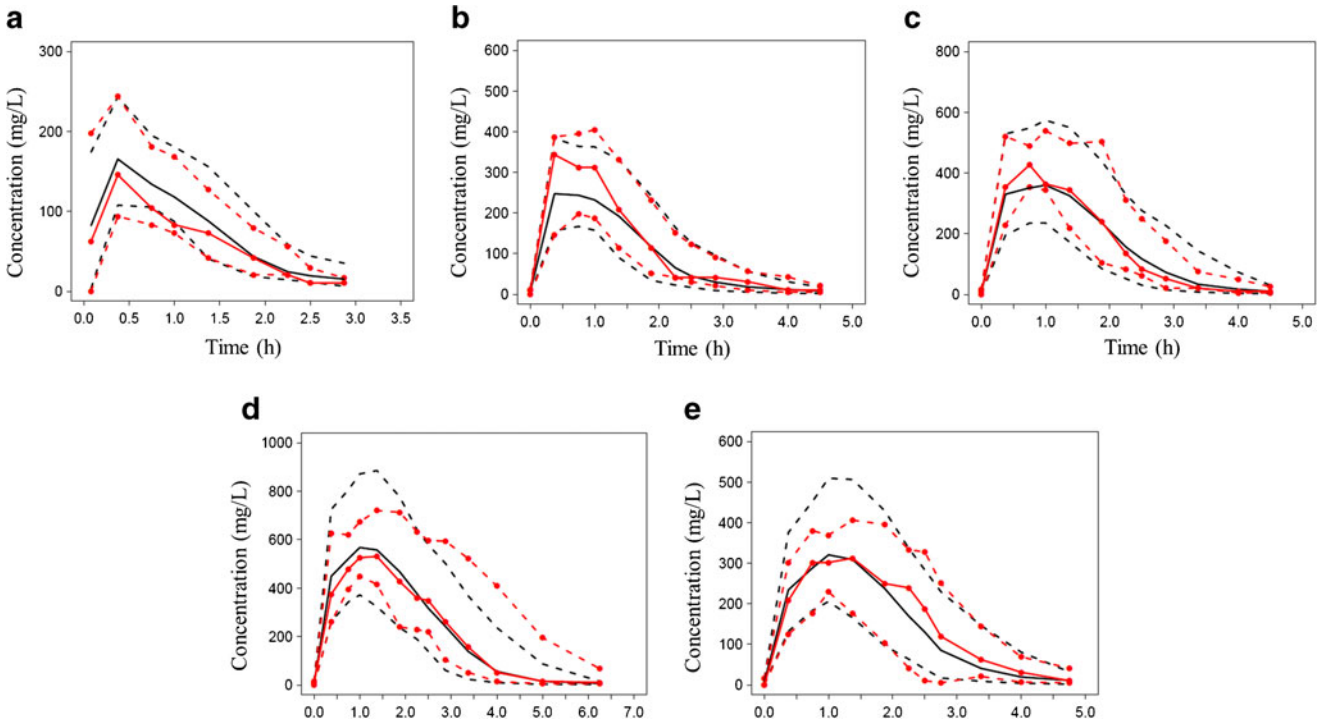

Fig. 4. VPCs for the final population PK model across the doses showing 10th, 50th and 90th percentiles of the observed and model predicted data. *Dashed dotted lines* and *solid dotted line* represent percentiles of the observed data (*red lines*), *dashed lines* and *solid line* represent percentiles from the model predictions (*black lines*). Subplots **a** to **d** are citrus-flavoured sports water preparation and subplot **e** is chocolate milkshake meal replacement preparation. The doses were (**a**) 192 mg/kg, (**b**) 291 mg/kg, (**c**) 395 mg/kg, (**d**) 573 mg/kg and (**e**) 500 mg/kg

moderate ketotic conditions (> 0.5 mmol/L (> 52.05 mg/L)), a mixed-order picture may become apparent. Tissue uptake of ketones is mainly facilitated by MCT proteins. This uptake is saturable in some tissues when the circulating blood ketone concentrations are high (41). The estimate of V in this study (population mean value, 12.5 L) was comparable to the literature-reported value (10 L) following intravenous administration using tracer compound (20). The maximum clearance (i.e. sum of first-order (CL) and maximum rate of capacity limited elimination (V_{max}/k_m)) observed in this study (96.7 L/h) were comparable to literature-reported clearance of BHB (112 L/h) that was estimated following intravenous administration of the tracer compound (20,21).

One of the factors that adds to the complexity of the PK of BHB is the endogenous production. The liver of a healthy adult is capable of producing up to 185 g of ketones (BHB + AcAc) per day during prolonged starvation (6). Normal production of ketones following an overnight fast in healthy adults is in the order of 30 to 60 g/day (22). Internal factors, such as pathophysiological conditions, and external factors, such as diet and intensity of physical work, influence the endogenous production. This can lead to highly variable basal concentrations of BHB across individuals. Endogenous input was included in the model to account for endogenous basal concentrations of BHB. Our estimate of the basal concentration for BHB in this study, 7.23 mg/L (0.07 mmol/L), was close to the literature reported value of 12.5 mg/L (0.12 mmol/L) (22). It is known from the literature that endogenous ketone production is suppressed during the post-absorptive phase, is affected by glucagon:insulin system, and by circulating blood ketones concentrations of > 3 to 5 mmol/L (6,42). Inclusion of negative feedback effects of circulating BHB on endogenous input improved the fit of the model. Occurrence of relatively large amounts of BLQ data, corresponding to approximately 13% of the total data, in the terminal phase indicated that negative feedback occurred in this study. Although mechanistically plausible and statistically significant (as observed in this study), the estimates of negative feedback effect (*SLP* and *INT*) had relatively poor precision in this study, and further studies are needed to confirm the quantitative mechanisms of feedback on production. We emphasise that the mechanism of feedback in this study needs to be interpreted with caution and requires further work to substantiate the process.

In the population PK model, it was observed that formulation affected F and $k_{afastsite}$ and dose affected F and $f_{slowsite}$. The estimate of covariate effect of dose on F had relatively poor precision (% RSE 144). This could be due to small sample size in this study, and it needs to be addressed in future studies with sufficiently large population. In total, five dose levels (four with the citrus-flavoured drink and one with the chocolate milkshake meal replacement preparation) were used (Table I). The citrus-flavoured sports water was a less viscous preparation compared to the chocolate milkshake

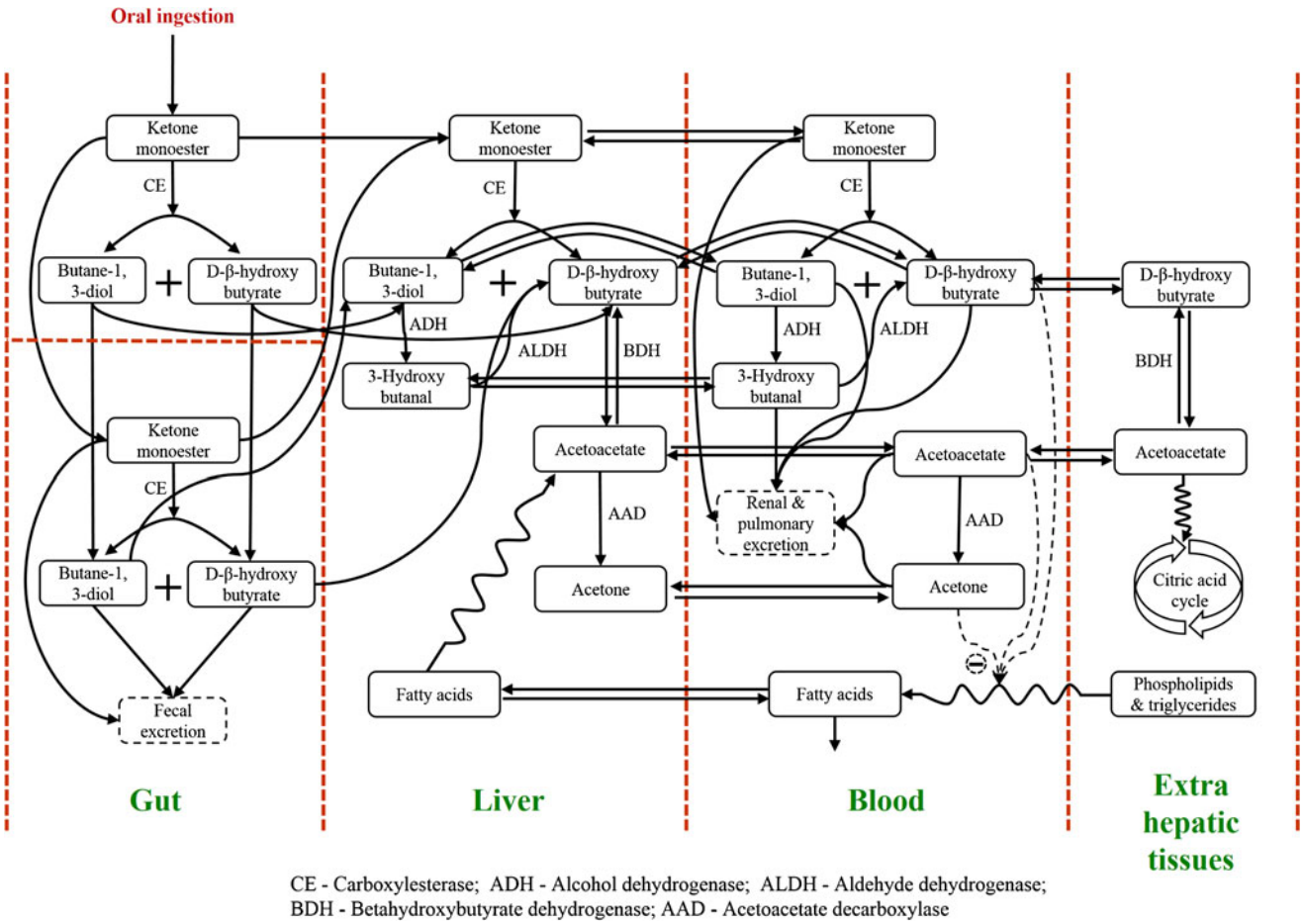

Fig. 5. Schematic representation of ketone monoester catabolism *in vivo*. *Solid continuous arrows* represent mass transfer/reaction/production, *dashed arrows* represent feedback process (*negative sign next to the dashed arrows* represents inhibitory feedback process) and *wiggly arrows* represent transduction process. Ketone monoester, upon oral ingestion is hydrolysed to butane-1,3-diol and BHB by carboxylesterases expressed throughout the gastrointestinal tract, liver and in blood. Butane-1,3-diol is oxidised sequentially, to produce 3-hydroxybutanal and BHB in the liver and blood. BHB is further metabolised to produce other ketones, namely, AcAc and acetone in the liver and blood. Endogenous ketones are produced in the form of AcAc in the liver from metabolism of fatty acids (breakdown products of phospholipids and triglycerides in the adipose tissue). Ketones in the blood circulation are taken up by extra hepatic tissues such as the brain, kidney, skeletal muscle and heart where they are used as energy source to produce ATP via citric acid cycle. Excess ketones in the blood that are not taken by tissues are either exhaled from lungs in the form of acetone or excreted as BHB and AcAc from the kidneys

meal replacement preparation. The chocolate milkshake was also larger in volume and contained fat, carbohydrate and proteins. Differences between these two formulations resulted in greater than 50% difference in exposure (estimate of F was 0.37 for chocolate milkshake meal replacement preparation compared to the citrus-flavoured drink). It was found that the fraction absorbed from the slow input site was dose-dependent and increased with the dose administered. Other influential covariates were LBW and sex. The effect of LBW on first-order clearance was not unexpected since lean tissues are considered to be a major source of metabolism of BHB and hence LBW is a direct measure of metabolic potential. The high value for the power coefficient (2.09) of LBW on first-order clearance should be reconfirmed in future studies with a larger population size. The mechanism for the influence of sex on V is unclear, as a size difference between males and females would be expected to be identified by LBW. This needs to be tested in future studies to determine a mechanism for this finding or to show that this finding is a statistical artefact of the data.

CONCLUSION

The population PK model for BHB developed in this study provided an acceptable description of the current data. It was found that the PK of BHB is complicated, and more work to determine and quantify mechanisms of absorption and elimination are required in future studies. Overall, this study forms an initial understanding of the mechanisms related to PK disposition of BHB.

ACKNOWLEDGEMENTS

Vittal Shivva was supported by a Postgraduate Scholarship, University of Otago, Dunedin, New Zealand.

Author Contributions P.J.C., K.C. and R.L.V. have contributed to the design and execution of the clinical study. V.S., I.G.T. and S.B.D. have contributed to the design and execution of the modelling and data analysis. V.S. has prepared the manuscript, and all authors have reviewed the manuscript.

COMPLIANCE WITH ETHICAL STANDARDS

Conflict of Interest The intellectual property covering the uses of ketone bodies and ketone esters are owned by BTG Ltd., the University of Oxford and the National Institutes of Health. Should royalties ever accrue from these patents, Kieran Clarke and Richard L Veech, as inventors, will receive a share of the royalties under the terms prescribed by each institution. Kieran Clarke is a non-executive director of TdeltaS Ltd, a company spun out of the University of Oxford to develop products based on the science of ketone bodies in human nutrition. All authors declare no other conflicts of interest.

REFERENCES

1. Veech RL, Chance B, Kashiwaya Y, Lardy HA, Cahill JGF. Ketone bodies, potential therapeutic uses. IUBMB life. 2001;51(4):241–7.
2. Harvey RAPD, Ferrier DR, Champe PC. Biochemistry. Philadelphia: Wolters Kluwer Health/Lippincott Williams & Wilkins; 2011.
3. Cahill JGF, Veech RL. Ketoacids? Good medicine? Trans Am Clin Climatol Assoc. 2003;114:149–63.
4. Cahill Jr GF. Starvation in man. N Engl J Med. 1970;282(12):668–75.
5. Mitchell GA, Kassovska-Bratinova S, Boukaftane Y, Robert MF, Wang SP, Ashmarina L, *et al*. Medical aspects of ketone body metabolism. Clin Invest Med. 1995;18(3):193–216.
6. Laffel L. Ketone bodies: a review of physiology, pathophysiology and application of monitoring to diabetes. Diabetes Metab Res Rev. 1999;15(6):412–26.
7. Freeman JM, Kossoff EH, Hartman AL. The ketogenic diet: one decade later. Pediatrics. 2007;119(3):535–43.
8. Henderson ST. Ketone bodies as a therapeutic for Alzheimer's disease. Neurotherapeutics. 2008;5(3):470–80.
9. Kashiwaya Y, Takeshima T, Mori N, Nakashima K, Clarke K, Veech RL. D-beta-hydroxybutyrate protects neurons in models of Alzheimer's and Parkinson's disease. Proc Natl Acad Sci U S A. 2000;97(10):5440–4.
10. Kashiwaya Y, Bergman C, Lee JH, Wan R, King MT, Mughal MR, *et al*. A ketone ester diet exhibits anxiolytic and cognition-sparing properties, and lessens amyloid and tau pathologies in a mouse model of Alzheimer's disease. Neurobiol Aging. 2013;34(6):1530–9.
11. Cox PJ, Clarke K. Acute nutritional ketosis: implications for exercise performance and metabolism. Extrem Physiol Med. 2014;3:17–7.
12. Lee CY. The effect of high-fat diet-induced pathophysiological changes in the gut on obesity: what should be the ideal treatment? Clin Transl Gastroenterol. 2013;4(7):e39.
13. Clarke K, Tchabanenko K, Pawlosky R, Carter E, Todd King M, Musa-Veloso K, *et al*. Kinetics, safety and tolerability of (R)-3-hydroxybutyl (R)-3-hydroxybutyrate in healthy adult subjects. Regul Toxicol Pharmacol. 2012;63(3):401–8.
14. Liederer BM, Borchardt RT. Enzymes involved in the bioconversion of ester-based prodrugs. J Pharm Sci. 2006;95(6):1177–95.
15. Satoh T, Hosokawa M. Structure, function and regulation of carboxylesterases. Chem Biol Interact. 2006;162(3):195–211.
16. Garber AJ, Menzel PH, Boden G, Owen OE. Hepatic ketogenesis and gluconeogenesis in humans. J Clin Invest. 1974;54(4):981–9.
17. Owen OE. Ketone bodies as a fuel for the brain during starvation. Biochem Mol Biol Educ. 2005;33(4):246–51.
18. Balasse EO. Kinetics of ketone body metabolism in fasting humans. Metabolism. 1979;28(1):41–50.
19. Cobelli C, Nosadini R, Toffolo G, McCulloch A, Avogaro A, Tiengo A, *et al*. Model of the kinetics of ketone bodies in humans. Am J Physiol. 1982;243(1):7–17.
20. Wastney ME, Hall SE, Berman M. Ketone body kinetics in humans: a mathematical model. J Lipid Res. 1984;25(2):160–74.
21. Hall SE, Wastney ME, Bolton TM, Braaten JT, Berman M. Ketone body kinetics in humans: the effects of insulin-dependent diabetes, obesity, and starvation. J Lipid Res. 1984;25(11):1184–94.
22. Balasse EO, Fery F. Ketone body production and disposal: effects of fasting, diabetes, and exercise. Diabetes Metab Rev. 1989;5(3):247–70.
23. Janmahasatian S, Duffull SB, Ash S, Ward LC, Byrne NM, Green B. Quantification of lean bodyweight. Clin Pharmacokinet. 2005;44(10):1051–65.
24. Abbott. Clinical Evaluation of a Faster, Smaller Sample Volume Blood ß-Ketone Test Strip Abbott Diabetes Care Inc. 2006. Available from: https://abbottdiabetescare.co.uk/images/uploads/documents/08_KII_white__paper.pdf Accessed 2 September 2013.
25. Guerci B, Benichou M, Floriot M, Bohme P, Fougnot S, Franck P, *et al*. Accuracy of an electrochemical sensor for measuring capillary blood ketones by fingerstick samples during metabolic deterioration after continuous subcutaneous insulin infusion interruption in type 1 diabetic patients. Diabetes Care. 2003;26(4):1137–41.
26. Forrow NJ, Sanghera GS, Walters SJ, Watkin JL. Development of a commercial amperometric biosensor electrode for the ketone D-3-hydroxybutyrate. Biosens Bioelectron. 2005;20(8):1617–25.
27. Bauer RJ. NONMEM users guide introduction to NONMEM 7.2.0. Ellicott City: ICON Development Solutions; 2011.
28. Beal S. Ways to fit a PK model with some data below the quantification limit. J Pharmacokinet Pharmacodyn. 2001;28(5):481–504.
29. Dansirikul C, Silber HE, Karlsson MO. Approaches to handling pharmacodynamic baseline responses. J Pharmacokinet Pharmacodyn. 2008;35(3):269–83.
30. Kumar VVP, Oscarsson S, Friberg LE, Isbister GK, Hackett LP, Duffull SB. The effect of decontamination procedures on the pharmacokinetics of venlafaxine in overdose. Clin Pharmacol Ther. 2009;86(4):403–10.
31. Karlsson MO, Holford N. A tutorial on visual predictive checks. Marseille: Population Approach Group Europe PAGE; 2008.
32. Bergstrand M, Hooker AC, Wallin JE, Karlsson MO. Prediction-corrected visual predictive checks for diagnosing nonlinear mixed-effects models. AAPS J. 2011;13(2):143–51.
33. Savic RM, Karlsson MO. Importance of shrinkage in empirical bayes estimates for diagnostics: problems and solutions. AAPS J. 2009;11(3):558–69.
34. Desrochers S, Dubreuil P, Brunet J, Jette M, David F, Landau BR, *et al*. Metabolism of (R, S)-1,3-butanediol acetoacetate esters, potential parenteral and enteral nutrients in conscious pigs. Am J Physiol. 1995;268(4 Pt 1):E660–7.
35. Jones AW, Eklund A, Kronstrand R. Concentration-time profiles of gamma-hydroxybutyrate in blood after recreational doses are best described by zero-order rather than first-order kinetics. J Anal Toxicol. 2009;33(6):332–5.
36. Halestrap AP, Price NT. The proton-linked monocarboxylate transporter (MCT) family: structure, function and regulation. Biochem J. 1999;343(Pt 2):281–99.
37. Gill RK, Saksena S, Alrefai WA, Sarwar Z, Goldstein JL, Carroll RE, *et al*. Expression and membrane localization of MCT isoforms along the length of the human intestine. Am J Physiol Cell Physiol. 2005;289(4):C846–52.

38. Broer S, Schneider HP, Broer A, Rahman B, Hamprecht B, Deitmer JW. Characterization of the monocarboxylate transporter 1 expressed in Xenopus laevis oocytes by changes in cytosolic pH. Biochem J. 1998;333(Pt 1):167–74.
39. Broer S, Broer A, Schneider HP, Stegen C, Halestrap AP, Deitmer JW. Characterization of the high-affinity monocarboxylate transporter MCT2 in Xenopus laevis oocytes. Biochem J. 1999;341(Pt 3):529–35.
40. Nosadini R, Avogaro A, Doria A, Fioretto P, Trevisan R, Morocutti A. Ketone body metabolism: a physiological and clinical overview. Diabetes Metab Rev. 1989;5(3):299–319.
41. Poole RC, Halestrap AP. Transport of lactate and other monocarboxylates across mammalian plasma membranes. Am J Physiol. 1993;264(4 Pt 1):C761–82.
42. Balasse EO, Neef MA. Inhibition of ketogenesis by ketone bodies in fasting humans. Metabolism. 1975;24(9):999–1007.